Daily cycle simulations of thermally stratified flows over forests

Avila, M.; Chávez-Arroyo, R. A.; Arnqvist, J.; Olivares-Espinosa, H.; Dellwik, Ebba

Published in:
Proceedings of the Wake Conference 2019

Link to article, DOI:
10.1088/1742-6596/1256/1/012003

Publication date:
2019

Document Version
Publisher's PDF, also known as Version of record

Daily cycle simulations of thermally stratified flows over forests

IOP Conf. Series: Journal of Physics: Conf. Series **1256** (2019) 012003 doi:10.1088/1742-6596/1256/1/012003

Daily cycle simulations of thermally stratified flows over forests

M Avila[1], R A Chávez-Arroyo[2], J Arnqvist[3], H Olivares-Espinosa[3] and E Dellwik[4]

[1] Barcelona Supercomputing Center, CASE Department, Barcelona, Spain
[2] National Renewable Energy Centre (CENER), Sarriguren, Spain
[3] Uppsala University Campus Gotland, Department of Earth Sciences, Wind Energy Section, 621 67 Visby, Sweden
[4] Technical University of Denmark, Department of Wind Energy, Roskilde, Denmark

E-mail: matias.avila@bsc.es

Abstract.

The aim of the present work is to obtain a better understanding of how to model the thermally stratified wind field over a forest during full diurnal cycles. The setup of the study assumes a horizontally homogeneous forest, with the objective of finding a simple and efficient way to model the canopy flow using time-dependent input data, obtained from measurements and mesoscale simulations. With this, new insights can be gained for future microscale modelling of complex forested terrains using mesoscale input data. In terrain without forest a diurnal cycle is commonly simulated by imposing time-dependent ground temperature. However, the presence of forests partially isolates the temperature at ground level from the flow above the canopy, making this common approach ineffective. This work proposes imposing the time-dependent net radiation at the forest canopy top to drive the thermal stratification changes along the diurnal cycle. To this end, several full days of simulation are driven by prescribing the net radiative heat flux balance measured on top of the canopy, together with a geostrophic pressure gradient. The advantage of the method is its simplicity and that the input data can be easily obtained from mesoscale modelling.

When compared to the observations at the Swedish site Ryningsnäs, the new method dramatically improves estimations of wind speed, wind direction and turbulent kinetic energy compared to simulations that only assume neutral stratification. Out of the variables studied, temperature and turbulent heat flux profiles were the ones that qualitatively followed the measurements the best, while wind speed and turbulent kinetic energy showed a larger disagreement.

1. Introduction

A key point for the assessment of wind energy efficiency is the accurate characterization of the resource in the planning of wind farms, requiring a careful determination of the micro-meteorological processes. Wind farms continue to be erected in high-latitude forested areas, where transient effects of thermal stratification strongly affect the turbulence levels, as well as wind profile and wind direction. The aim of the present work is to obtain a better understanding of how to simulate full diurnal cycles of thermally stratified wind field over forested sites in microscale models, for wind energy assessment.

When simulating a daily cycle in a wind farm without forest, a common approach is to prescribe a time-dependent temperature at the ground, which becomes the driver of the daily cycle simulation (e.g. [1, 2] and references therein). However, the presence of forests causes the temperature at ground level to be partially isolated from the wind above the canopy. Therefore, imposing a time-dependent ground temperature does not influence the wind temperature and velocity above the forest to produce their variation at the desired rate and magnitude. Consequently, this is an ineffective methodology to drive a daily cycle simulation over forested terrain.

Recently, various models have been used to simulate and compare the wind over forested and moderately complex terrain [3]; nevertheless none of these models was able to represent thermally stratified flows. In the last several years, numerical simulations models [4, 5] have become increasingly applied to canopy flows with thermal stratification over homogeneous terrains. When a tree coverage is included, forests have been simulated for different stability conditions [6, 5, 7], assuming that radiation penetrates the canopy, as suggested by Brown and Covey [8]. During daytime/nighttime radiation warms/cools the foliage which, in turn warms/cools the air in contact with it. Models used in previous works were conceived to solve quasi-steady flows.

The present work develops a new and simple methodology to drive diurnal cycles of thermally stratified wind over forested regions. Several full days of simulation are driven by prescribing the net radiative heat flux at the top of the canopy as well as the geostrophic pressure gradient, which are obtained from field measurements and mesoscale simulations, respectively. The simulated wind velocity, temperature, turbulent kinetic energy results are compared against field measurements from a site in the South-East of Sweden [9, 10].

Boy et al [11] developed a more complex model over homogeneous and flat terrain, where the daily cycle simulations were also driven by net radiative heat flux. The methodology presented in this work is simpler, and uses less parameterizations. The present model is an early stage, aimed to represent an acceptable compromise between physical representation and model complexity, with future goal to simulate complex phenomena such as the reproduction of diurnal cycles over nonhomogeneous forests and complex terrains. The proposed model is based on a simplified approach that, in light of the compromises provides a fair prediction of the daily temperature, velocity and turbulent kinetic energy fluctuations.

2. Physical model and governing equations of thermal flow over a forest

The unsteady Reynolds-Averaged Navier-Stokes (RANS) equations are solved to obtain the mean wind flow. These equations make use of the Reynolds decomposition to separate the velocity and potential temperature fields into time-averaged and fluctuating components, $\mathbf{u} = \overline{\mathbf{u}} + \mathbf{u}'$ and $\theta = \overline{\theta} + \theta'$. We make use of the Boussinesq approximation and gradient diffusion hypotheses, in which the Reynolds stresses and the turbulent heat flux are parameterized as a function of an eddy viscosity ν_t and the rate of strain tensor S (the symmetric component of the gradient of time-averaged velocity, i.e. $S_{ij} = 0.5\,(\partial\overline{u}_i/\partial x_j + \partial\overline{u}_j/\partial x_i)$, where x_i are the spatial coordinates) in the momentum equation, and the time averaged temperature gradient $\nabla\overline{\theta}$ in the energy equation.

The Reynolds-averaged mass, momentum and energy conservation equations are

$$\nabla \cdot \mathbf{u} = 0 \tag{1}$$

$$\frac{\partial \mathbf{u}}{\partial t} + \mathbf{u}\cdot\nabla\mathbf{u} - \nabla\cdot(2\nu_t S) + \nabla p + c_d A|\mathbf{u}|\mathbf{u} + f_c\,\mathbf{e}_z \times (\mathbf{u} - \mathbf{u}_g) + \alpha\mathbf{u} = -\mathbf{g}\frac{\theta}{\theta_0} \tag{2}$$

$$\frac{\partial \theta}{\partial t} + \mathbf{u}\cdot\nabla\theta - \nabla\cdot\left(\frac{\nu_t}{\sigma_\theta}\nabla\theta\right) = \frac{\partial q_r}{\partial z} \tag{3}$$

where the simulated fields are the wind velocity $\mathbf{u}$, the pressure p and the potential temperature θ. The fifth term in Eq. (2) is the drag force exerted by the canopy, where c_d is the drag coefficient, taken as $c_d = 0.2$ [12] and A is the plant area density (PAD) ($\mathrm{m}^2/\mathrm{m}^3$), accounting for leaves, stems and branches. The sixth term in Eq. 2 is the Coriolis force, where the Coriolis parameter is $f_c = 2\Omega \sin\lambda$ (with Ω the earth's rotation rate and λ the latitude) and $\mathbf{e}_z$ the local unit vector pointing in the vertical direction z. The geostrophic velocity $\mathbf{u}_g$ is related to the geostrophic pressure gradient driving the flow, as $\nabla p_g = 2\Omega \times \mathbf{u}_g$. The seventh term is added to the model in order to damp velocity oscillations in the free atmosphere [13], activated when the geostrophic pressure gradient is time-dependent. The term on the right hand side is the buoyant term, where θ_0 is a reference temperature and $\mathbf{g}$ is the gravity force. In the energy equation (3), σ_θ is the turbulent Prandtl number. On the right hand side of Eq. (3), q_r represents the net radiative flux, defined as positive when pointing downwards; thus, q_r yields the difference between downward and upward radiation fluxes, becoming positive during daytime and negative during nighttime. Above the canopy q_r is assumed as uniform, so the heat source term $\partial q_r/\partial z$ is ignored. For a canopy of uniform height z_c, the radiative heat flux inside the canopy can be described [8, 6] by:

$$q_r(z,t) = Q(z_c,t)\exp\left(-\eta PAI(z)\right), \qquad PAI(z) = \int_z^{z_c} A(z)dz, \tag{4}$$

where $Q(z_c)$ is the net radiation flux at the top of the canopy $z = z_c$, which decreases inside the layer of trees depending on the cumulative downward plant-area index $PAI(z)$ and the extinction coefficient of light η (assumed to have a constant value $\eta = 0.6$ as in [5, 6]).

The radiative heat flux profile is modeled in the same way for stable and unstable conditions (day and night) via the sign of $Q(z_c)$. To be noted here is that there is no heat storage in the canopy itself. Forest temperature is always in balance with air temperature through direct release of absorbed radiation through Eq. (3). This assumption rules out a time lag between forest and air temperature which may be present in reality.

The RANS model is closed using the k-ε model of Sogachev et al. [4], which was developed for canopy flows in a thermally stratified atmosphere. This model is implemented in Fortran90 as a 1D single column model. An important constraining approximation is the absence of moisture in the primitive equations which will cause errors when applying the model to periods with Bowen ratio (ratio of sensible to latent heat flux) much lower than unity.

3. Quasi-steady simulation; relevance of the thermal boundary condition at ground level

The first simulation is a thermally stratified canopy flow, similar to the very stable case run by Nebenführ and Davidson [5]. The canopy has a height $z_c = 20$ m and a uniform plant area density (PAD) of 0.3 m^{-1} which is representative of the forested Ryningsnäs site; therefore the plant area index (PAI) is $\int_0^{z_c} A(z)dz$=6. Two simulations are performed, using different boundary conditions at the wall: one with zero turbulent heat flux at the bottom surface and the other with a constant ground temperature $T_{wall} = 275$ K, using Monin-Obukhov similarity theory to find the turbulent heat flux at the lowest level. The Coriolis parameter is set to $f_c = 1.22 \cdot 10^{-4}$ s^{-1}, corresponding to a latitude of 57 degrees, and the geostrophic velocity magnitude is set to $|\mathbf{u}_g| = 17.5$ m/s. This corresponds to a wind speed of ~ 8 m/s at a height of 80 m. The initial condition is the steady state solution of the model for the neutral canopy. The initial potential temperature is uniform until a height of 400 m, imposing a capping inversion of 5 K/km above this height. The obtained wind profiles are compared after 8 hours of applying a constant radiative cooling of $Q(z_c) = -0.016Km/s$ at the top of the canopy, which is equivalent to ~ 200 $\mathrm{W/m}^2$. After 8 hours of cooling (a long winter night) a quasi-steady solution is obtained for all fields, except the temperature, which continues decreasing. This aspect is discussed below.

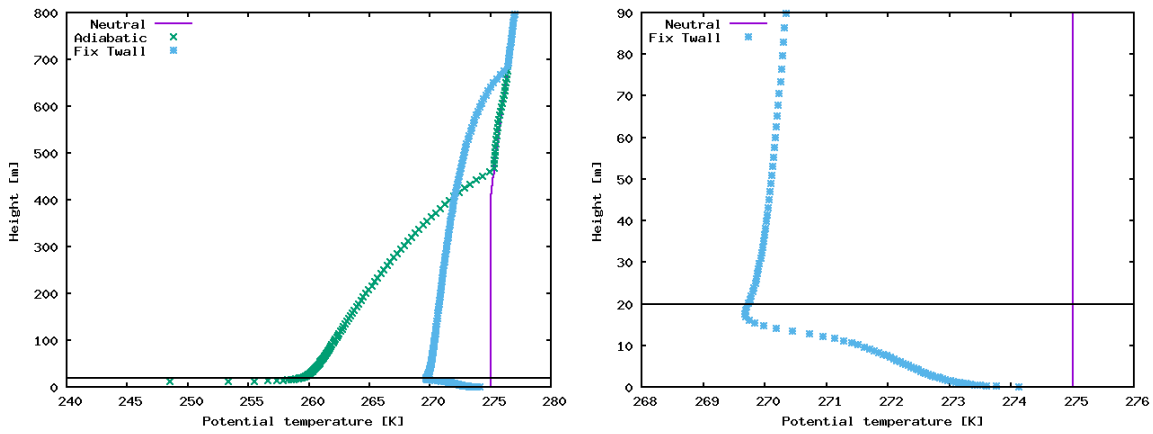

Figure 1. Potential temperature profile resulting from fixing the temperature at the wall (blue stars) and when there is no exchange of heat with the ground (green marks). Solid line shows the temperature profile of the neutral case. A zoom-in is shown on the right figure to observe the temperature profile near the canopy region.

Fig.1 shows the potential temperature profiles after 8 hours of cooling. The canopy releases radiative heat, cooling the surrounding air. For a constant surface temperature, the ground heats the canopy from below via turbulent heat flux so that the minimum temperature is found close to the top of the canopy. The simulated surface acts as a source of heat; without it, the simulated temperature of the canopy decreases with time, as seen in Fig.1. Although the imposition of zero turbulent heat exchange at ground level was used in [5, 6], here (e.g. Fig. 1) we are reminded that such an imposition is not a realistic boundary condition. This effect is formally seen from a perspective of global energy conservation, discussed below.

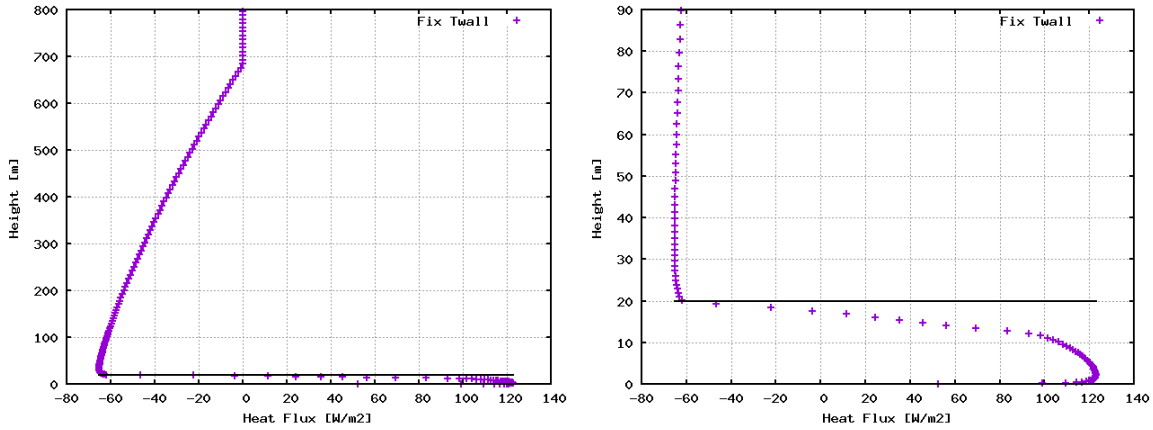

Figure 2. Upward turbulent heat flux profile when fixing wall temperature. On the right, a zoom-in near the canopy region.

Global energy Conservation. When integrating the energy equation (3) from the ground to the top of the domain ($z = H$), the following expression is obtained for the integral temperature

variation:

$$\frac{\partial}{\partial t}\int_0^H \theta \mathrm{d}z = \overline{\theta' w'}_{ground} + Q(z_c)\left(1 - \exp\left(-\eta PAI\right)\right) \tag{5}$$

where $\overline{\theta' w'}_{ground}$ is the turbulent heat flux at ground level. Therefore, for a constant value $Q(z_c)$ the integral potential temperature can reach a steady state value only if the turbulent heat flux at ground level balances the net radiative heat flux absorbed or emitted by the canopy $Q(z_c)\left(1 - \exp\left(-\eta PAI\right)\right)$. When zero turbulent heat flux is imposed at the bottom surface, $\overline{\theta' w'}_{ground} = 0$, the temperature will be always changing because the net radiative heat flux emitted by the canopy is not balanced at ground level.

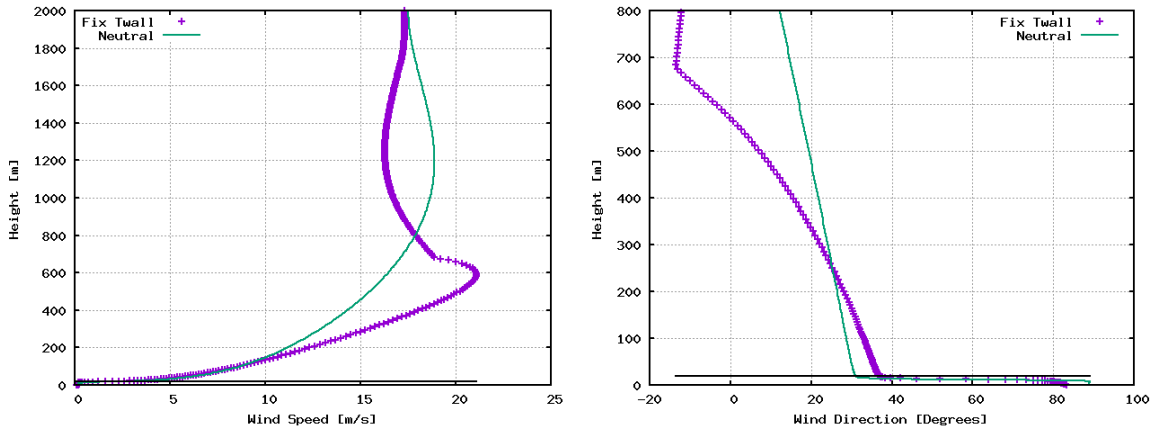

Figure 3. Wind speed (left) and wind direction profiles (right) for the neutral case (solid line) and for the stably stratified case when fixing the wall temperature (identified as "Fix Twall")

Fig. 2 shows the upward turbulent heat flux after 8 hours of cooling. When the temperature is fixed at ground level, the turbulent heat flux points upwards inside the canopy, changing its direction and pointing downwards above the canopy top. As the modeled canopy is colder than the ground, heat flux is removed from the ground to balance the radiation heat being lost by the canopy. In the stably stratified case, the turbulent heat flux above the canopy leads to a shallower boundary layer than in the neutral case. This feature is observed in Fig. 3, which shows the wind velocity and wind direction profiles after 8 hours of radiative cooling. The wind direction turns 90 degrees inside the canopy with regard to the free atmosphere. This occurs because inside the canopy the wind direction is aligned with the geostrophic pressure due to the low wind speed inside the highly dense forest. Fig.4 shows the turbulent kinetic energy (TKE) and shear stress profiles for the neutral and stably stratified atmosphere. The obtained TKE value depends on the C_μ parameter in the k-ε equations, which is set to $C_\mu = 0.0333$ in this paper to give a reasonable TKE level, as concluded in [3]. As expected, lower values for the TKE and the shear stress are obtained for the stable stratification. The TKE and shear stress have very low values inside the canopy, reaching its maximum just above the canopy height.

4. Diurnal cycle simulation, comparison against field measurements.

A diurnal cycle simulation is performed from net radiation measurements at the Ryningsnäs site in Sweden [9]. The obtained wind results are later compared against field measurements of turbulent fluxes and mean vertical profiles [9, 10]. The average forest height at the site is 20 m. The daily cycle is driven by the net radiation, which is measured at a height of 40 m above ground level. For the following study, a period of 9 days was chosen where the diurnal cycle

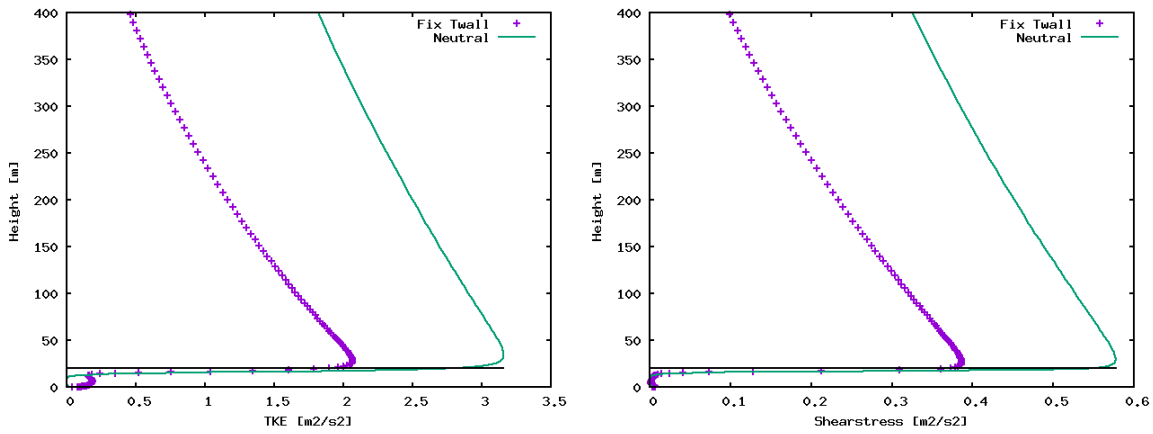

Figure 4. TKE (left) and shear stress profiles (right) for the neutral case (solid line) and for the stably stratified case when fixing wall temperature (labeled Fix Twall) .

was dominated by radiative forcing, i.e. mostly clear sky conditions. The simulation starts at midnight. The measured radiative heat is incorporated to the model as radiative heat at canopy height $Q(z_c, t)$ along 9 days of simulation. The Coriolis parameter is set to $f_c = 1.22 \cdot 10^{-4}$ s^{-1}, corresponding to a latitude of 57 degrees. The geostrophic pressure gradient (Fig.7) is obtained after running the mesoscale Weather Research and Forecasting (WRF) model driven by ERA5 reanalysis data at the location where field measurements where performed. The geostrophic pressure gradient is modeled as uniform in height and time dependent. The PAD $A(z)$ has a profile resembling a tree with a more dense region and a rather sparse trunk space, modeled using the empirical form from [14]. The profile has a PAI $\int_0^{z_c} A(z)dz = 3$. The actual forest at the site is dominated by evenly aged scots pines, making the PAD profile suitable, as explicitly concluded in [14]. Fig. 5 shows the PAD profile $A(z)$ of the modeled forest.

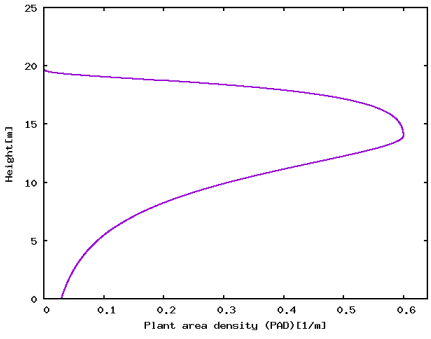

Figure 5. Plant area density profile $A(z)$ of the modeled forest.

The temperature at ground level is fixed to a constant value of 282 K. This value is representative of the averaged temperatures measured close to ground level. Monin-Obukhov similarity theory is used for temperature and velocity, which relates the shear stress/turbulent heat flux at ground level with the wind velocity/temperature at a distance $z_1 = 0.1$ m from the surface. It is assumed that the ground temperature does not change along the simulation days due to the partial insulation produced by the forest. The initial velocity profile is the solution of neutral flow, with a geostrophic wind speed of 9 m/s, The initial potential temperature profile is

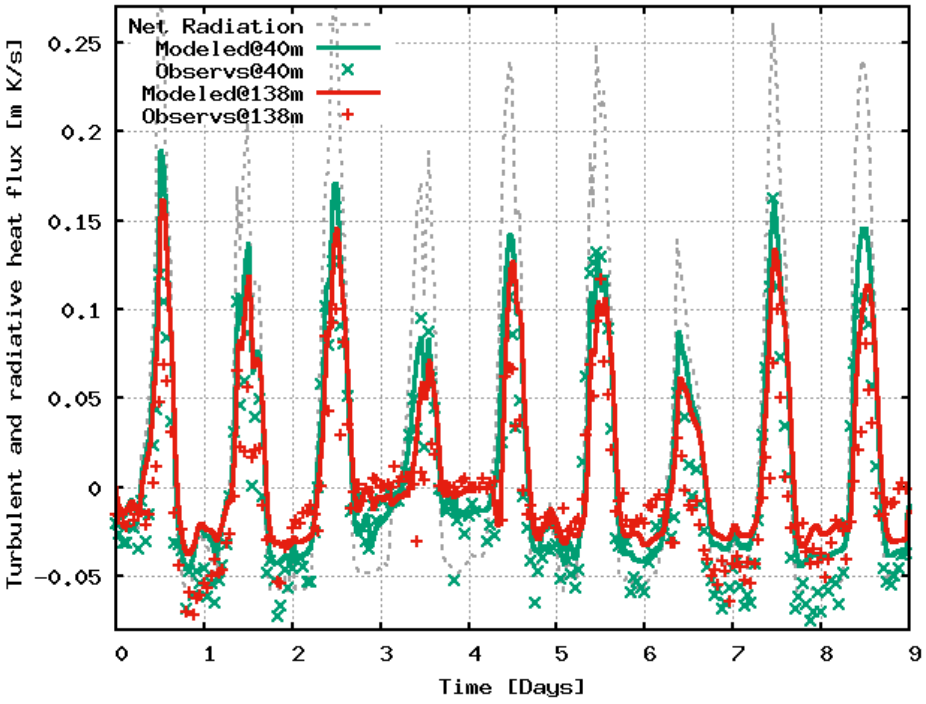

Figure 6. Radiative heat flux measured at 40m above ground level (dashed line), which is imposed to run the simulation. Observed and modeled turbulent heat flux $\overline{w'\theta'}$ also shown, both at 40 m and 138 m above ground level.

constant until a height of 700 m. From 700 m to the top of the domain ($z = 3000$ m) a capping inversion with a slope of 5 K/km is prescribed. The initial capping inversion is necessary to control the height of the Planetary Boundary Layer (PBL). Without this initial profile, the height of the PBL would go beyond the upper limit of the domain during daytime, when the atmosphere is convective.

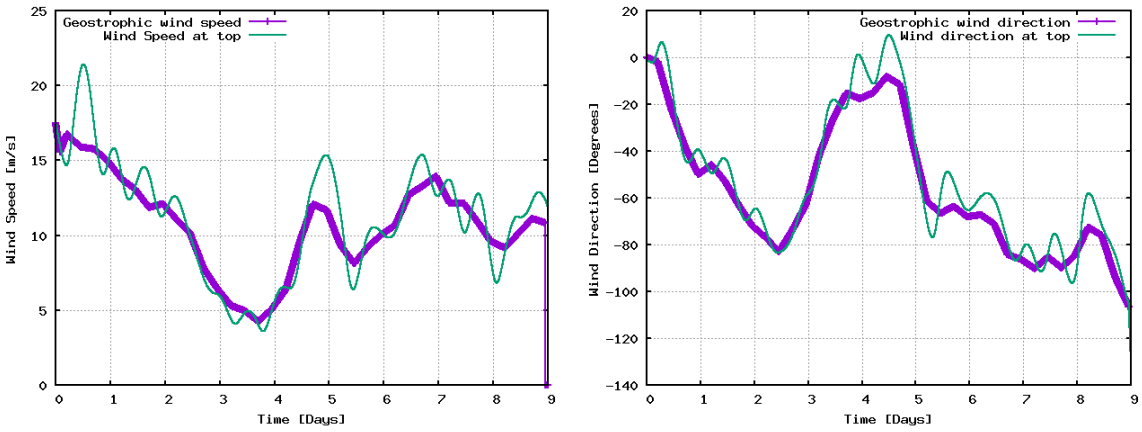

Figure 7. Input geostrophic wind speed (left) and direction (right) together with the simulated wind speed and direction at the free atmosphere when using a damping term.

Fig. 6 shows the time series of radiative heat flux divided by the specific heat per unit volume ($\rho c_p = 1232.9$ J/(m^{3}K)), which has negative values during the consecutive clear nights. The simulation starts at midnight, so the days displayed in all figures start also at midnight. This figure also shows the observed and modeled turbulent heat flux (Reynolds averaged vertical velocity and temperature fluctuations $\overline{w'\theta'}$) along the nine days of simulation at two different heights above ground level, $z = 40$ m and $z = 138$ m. It is important to keep in mind that the model does not take into account the effect of latent heat. This fact is considered a source of error since in reality the response to the net radiative heat flux is partitioned between latent and sensible heat flux, while in the model only the latter is accounted for. Still, a fair agreement is seen between the observed and simulated values. The relative differences between the modeled and observed heat fluxes are larger during nighttime than during daytime. It can also be noticed that the absolute values are larger at the lower height of 40 m than at $z = 138$ m. This finding agrees with the shape of the heat flux profile in the quasi-steady case in Fig. 2. The turbulent heat fluxes during nights 3 and 4 (simulation time around $t = 3$ days and $t = 4$ days), obtained at the measuring heights of 138 m and 40 m, show a significant reduction with height. This finding suggests that the depth of the PBL is around or less than 138 m, implying a very stable atmosphere during these nights. The boundary layer height during these nights is further discussed in section 4.1.

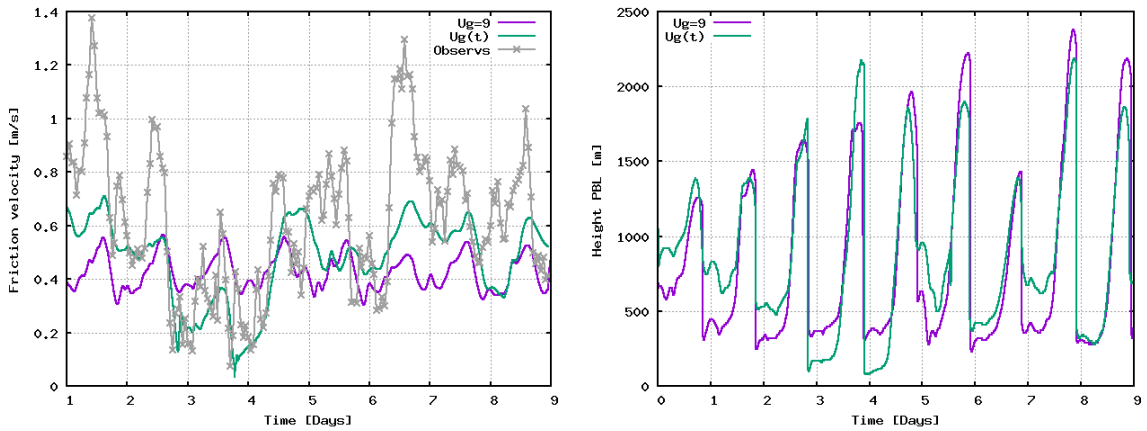

Figure 8. Observed and modeled friction velocity at 40 m height (left) and modeled temporal evolution of the height of the PBL (right). The model has been run setting a constant geostrophic wind speed of $U_g = 9$ m/s as well as by setting the time dependent geostrophic velocity $U_g(t)$.

Fig. 7 shows the geostrophic wind speed and direction along the 9 days of simulation. These velocities are shown together with the input geostrophic wind speed $|\mathbf{u}_g(t)|$ and its direction, extracted from the mesoscale model. The mismatch between free and geostrophic velocities are due to the inertial oscillations naturally appearing in the free atmosphere due to Coriolis force and the absence of friction [15]. The damping term in the momentum equation (2) is used to reduce the inertial oscillations. The damping coefficient has a value $\alpha = 10^{-5}$ s^{-1} above a height of 1000 m, decreasing linearly to zero at the ground level [13]. The maximum value of α is chosen to be one order of magnitude lower than the Coriolis parameter f_c, having a small influence on the equilibrium balance between pressure gradient and Coriolis force in the free atmosphere.

The boundary condition imposed at the top ($z = 3000$ m) is zero shear stress, zero vertical velocity and null turbulent heat transport $\overline{\theta' w'}$. When an horizontal wind velocity is prescribed at the top of the domain, an artificial mixing length generates from the top, modifying the wind profile at the free atmosphere. When imposing a time-dependent pressure gradient, the initial

velocity profile at time $t = t_0$ in the free atmosphere must be uniform and balanced with the initial pressure gradient. Hence, $\nabla p_g(t_0) = f_c \mathbf{e}_z \times \mathbf{u}(t_0)$ above the PBL to avoid the presence of highly fluctuating spatial and temporal oscillations of wind velocity in the free atmosphere.

4.1. Wind time series

The days displayed in all figures start at midnight. Fig. 8 shows the observed friction velocity, determined as $(-\overline{u'w'})^{1/2}$ from the 40 meter sonic, where u and w are respectively the horizontal and vertical wind velocity components. The observed friction velocity shows larger variations than the modeled friction velocity. When the pressure gradient is set as constant and uniform (labeled as "Ug=9"), the obtained friction velocity variations are only due to thermal stability changes between day and night, varying between 0.3 m/s and 0.57 m/s. When the pressure gradient is modeled as time-dependent (labeled as "Ug(t)") the friction velocity presents larger variations due the induced wind speed variations.

Fig. 8 shows the evolution of the height of the boundary layer when the pressure gradient is held constant (labeled "Ug=9") and when the pressure gradient is time-dependent (labeled "Ug(t)"). The height of the PBL is calculated as the lower height where the shear stress drops below 5% of the value at canopy height [16]. Fig. 8 shows that the boundary layer height drops every day just before midnight. Fig. 6 and Fig. 8 show that for the nights 3 and 4 (simulation time around $t = 3$ days and $t = 4$ days), both the heat flux and the shear stress point towards a very shallow boundary layer. The strong stratification during these nights is due to a combination of low geostrophic wind speed and negative radiative balance. As it can be seen in Fig. 8, the simulation with constant geostrophic wind speed yields a nocturnal boundary layer height that remains rather constant for the duration of the computation, while the simulation with varying geostrophic wind speed produces a boundary layer whose height follows the variation of the geostrophic wind speed. Hence, the modelling of a time dependent pressure gradient has an important effect.

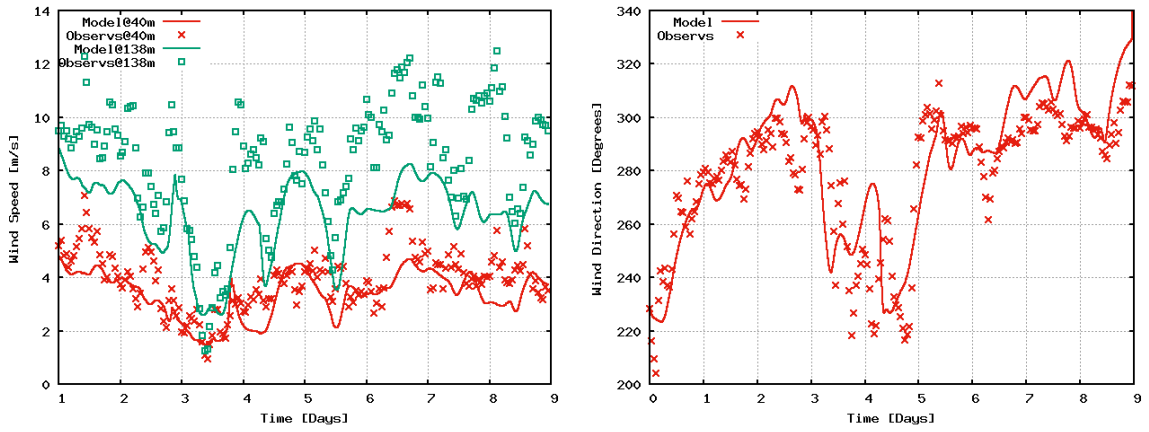

Figure 9. Modeled and observed wind speed at 40 m and 138 m above ground level (left). Observed and modeled wind direction at 138 m agl (right)

Fig. 9 shows the observed and modeled wind speeds at two different heights, $z = 40$ m and $z = 138$ m. While at $z = 40$ m the modeled wind speed is closer to observations, the agreement between simulated and measured wind direction is very similar at both heights, therefore, only the comparison of wind direction at $z = 138$ m is shown on Fig. 9 (right).

Fig. 10 shows the observed and predicted potential temperatures at heights $z = 40$ m and $z = 138$ m. The simulated temperatures show a similar trend during day and night than the

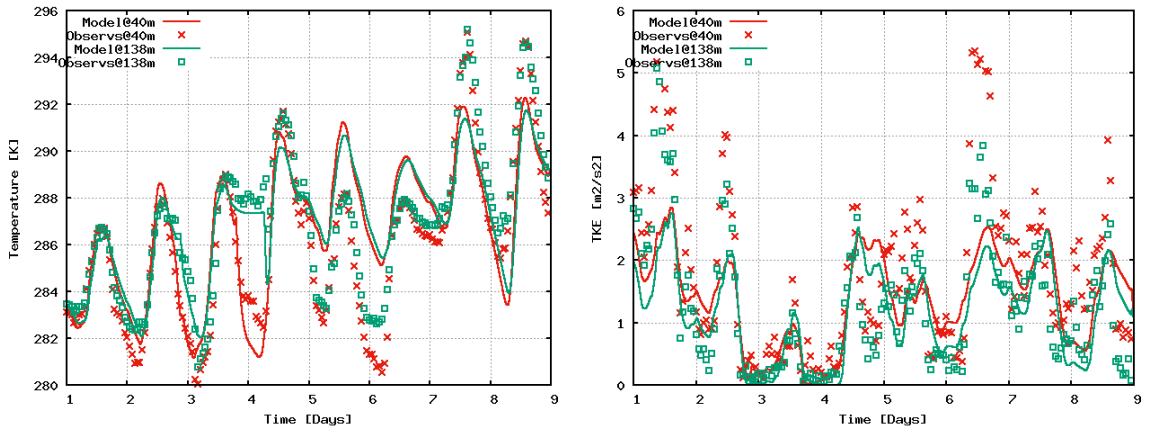

Figure 10. Modeled and observed temperatures (left) and turbulent kinetic energy (TKE) (right) at two different heights, 40 m and 138 m above ground level.

field measurements, having very similar variations. The obtained temperature variations are a consequence of prescribing only the radiation $Q(z_c, t)$ at canopy height, neglecting any effects of horizontal advection. Any effect of nighttime drainage currents is missed by the model, since it is single column. As shown by [17] nocturnal drainage flow can be an important component in canopies. Still, the obtained temperature is in general agreement with measurements at the two heights considered. Fig. 10 also shows the observed and modeled turbulent kinetic energy (TKE) at $z = 40$ m and $z = 138$ m. The modeled TKE is obtained when solving the TKE (k) equation of the k-ε model. The simulated TKE exhibits similar temporal trends and has similar values as the measured TKE during much of nighttime. However the measured TKE is ≈ 50 to 200% larger during daytime. The modeled TKE value depends on the C_μ parameter of the k-ε model, which is set to $C_\mu = 0.0333$ in the present work to obtain a reasonable TKE level [3]. The TKE is underpredicted during daytime, maybe due to the difficulty of modelling thermally stratified conditions using RANS models [18]. The wind speed at $z = 138$ m is underpredicted during nighttime, as was the nocturnal velocity gradient, as shown in section 4.2. Similar results were derived by Sogachev et al. [19]. They showed that even if the model can provide simulated temperature and heat flux comparable with measurements, it is still difficult to simulate wind speed and friction velocity values comparable to measured ones. It is clearly indicated that momentum and temperature have different footprints (temperature is not directly affected by pressure gradients) and this fact is not captured by the model.

4.2. Wind profiles

Fig. 11 shows the simulated and observed temperature profiles at times $t = 72$ h (midnight), $t = 84$ h (noon) , $t = 88$ h (4 p.m.) and $t = 96$ h (midnight). The profiles are selected along the 4^{th} day of simulation because it has a very strong thermal stability and low nocturnal PBL height (Figs. 8 and 6). The imposed constant temperature at ground level $T_w = 282$ K is not satisfied by observations. However, the shape of the obtained profiles matches quite well the trend of the temperature measurements. On Fig. 11 it is shown that temperature changes are mostly confined to the lower part of the domain. During the night the simulation gets a minimum temperature close to the top of the tree, however the field measurements show that the minimum temperature is at ground level. At noon the maximum of the simulated and observed temperature is found inside the canopy. The differences between the simulated and modelled temperature gradients might be affected by topography, which is not completely flat, and by

drainage currents [17], which are missed by the model.

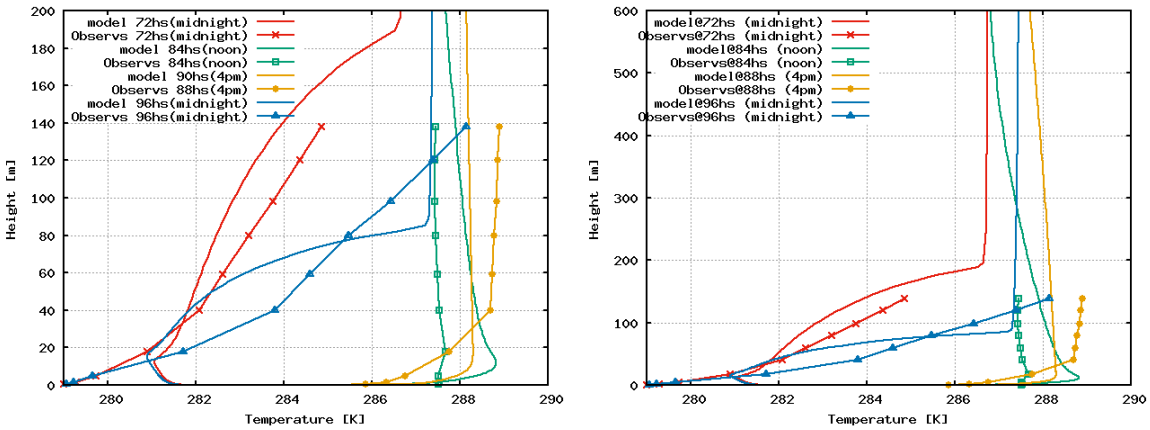

Figure 11. Observed and modeled temperature profiles at t=72 h (midnight), t=84 h (noon), t=88 (4 p.m.) and t=96 h (midnight). Results up to 200 m (left) and z=600 m (right)

Fig. 12 shows the obtained and observed wind profiles along the 4^{th} day of simulation, at times $t = 72$ h (midnight), $t = 84$ h (noon) , $t = 88$ h (4 p.m.) and $t = 96$ h (midnight). It is observed how the model captures the low level jet at midnight. The jet core in the model is at 170 m height at midnight (72 h) and as low as 75 m the following midnight. The measurements do not show a low level jet below 138 m, which indicates that the nocturnal boundary layer height is too low in the model. However, within the nocturnal boundary layer, the modelled and observed wind speed gradient is of similar magnitude, especially at 96 h. The strong differences in the velocities between day and night are mainly due to thermal stratification effects. Fig. 12 shows that the wind velocity above the PBL height has much lower variations than the wind velocity inside the PBL, stating that geostrophic pressure gradient has a small effect in the nocturnal velocity gradients.

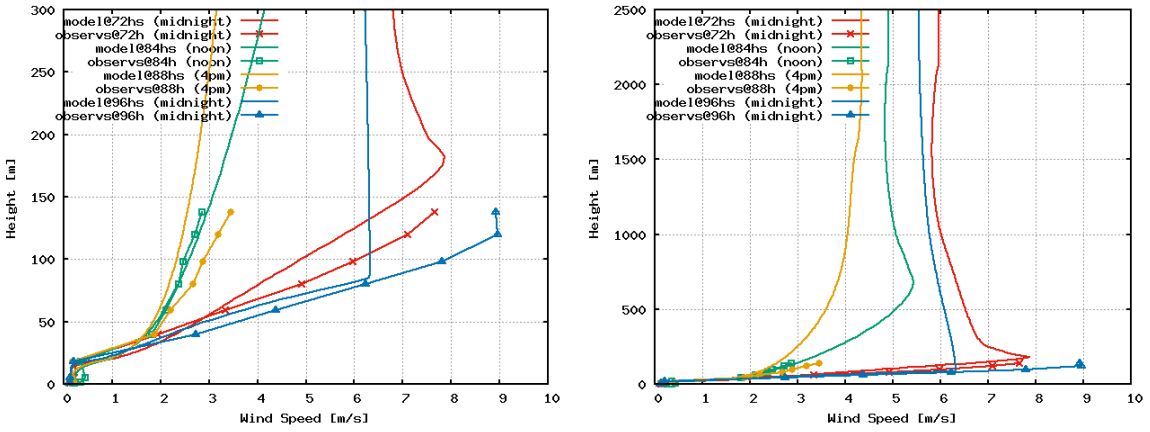

Figure 12. Observed and modeled velocity profile at t=72h (midnight), t=84h (noon), t=88 (4pm) and t=96h (midnight). Zoom up to 300 m height (left) and all domain (right)

5. Conclusion

In this work, a new methodology to run daily cycle simulations of thermally stratified flows over forests has been developed and tested. The simple method of driving the model with net radiative flux on the top of the canopy, while omitting any heat storage by the canopy itself, was shown to provide diurnal cycles of wind, temperature and turbulence, that qualitatively agreed with measured equivalents. The results were an improvement in comparison with running strictly neutral conditions, but some aspects could be improved. The nighttime turbulent heat flux was underestimated by the model, as was the nocturnal velocity gradient. At the same time, nocturnal boundary layers were too shallow and nocturnal levels of TKE too low. Underestimation of nighttime boundary layer height and heat flux suggests that the level of TKE may be to blame, but on the other hand nighttime levels of friction velocity were in better agreement with the measured values, indicating that the turbulence closure may need to be studied in more detail. The RANS equations were closed with the k-ε turbulence model. More elaborated RANS closures, or large eddy simulation (LES) could be used to see if the obtained wind profiles get closer to observations.

Furthermore, the model was run in a dry state, and as single column, meaning that any effects of horizontal temperature advection and latent heat flux is non-existent in the model. The chosen measurement period was selected to have a large amplitude of the net radiation as well as semi-stationary wind speed and direction, and while the measurement data was not filtered to specifically exclude periods of small latent heat fluxes or transient ambient temperatures, those effects were not studied and the impact of moisture and advection [2] should be considered for future studies. The latent heat flux generally is of the same order as the sensible heat flux during spring and autumn, but varying with latitude and forest type [20]. For future work,it will thus become important to develop strategies to account for the latent heat, for example by including a moisture equation, or simply by adjusting the incoming radiation by the use of climatological values for the Bowen ratio.

To summarize, the work presented in this study represents a minimal approach to implement transient stratified flows over forested terrain in CFD models. The simple method of using net radiation at the top of the canopy to drive the diurnal cycle evolution in micro-scale models has been shown to be viable. Net radiation is readily available from meteorological reanalysis and is easy to measure. The results obtained with this single column model suggest that the method is a reasonable compromise between adequate physical representation and simplicity of implementation. As such it is a possible way forward to achieve higher penetration of physically sound CFD models in wind energy applications, such as wind resource prediction, load modelling and wake modelling. A future implementation in a 3D solver will be useful to simulate the wind over forested and complex terrain.

Acknowledgments

This work has been partially supported by the New European Wind Atlas ERA-NET PLUS Project (NEWA, FP7-ENERGY.2013.10.1.2, European Commissions grant agreement 618122). Part of this work was conducted within STandUP for Wind, a part of the STandUP for Energy strategic research framework. Matias Avila and Roberto Chavez strongly thank Stefan Ivanell and Hugo Olivares-Espinosa for their support to conduct a research stay at Uppsala University Campus Gotland, the ensuing welcome and fruitful discussions.

References

[1] Barcons J, Avila M and Folch A 2017 *Wind Energy* 1–16
[2] Rodrigo J S, Arroyo R C, Gancarski P, Guillén F B, Avila M, Barcons J, Folch A, Cavar D, Allaerts D, Meyers J and Dutrieux A 2018 *Journal of Physics: Conference Series* **1037** 072030
[3] Ivanell S, Arnqvist J, Avila M, Cavar D, Chavez-arroyo R A, Olivares-espinosa H, Peralta C, Adib J and Witha B 2018 *Wind Energy Science Discussions* **20**

[4] Sogachev A, Kelly M and Leclerc M 2012 *Boundary-Layer Meteorology* **145** 307–327 ISSN 0006-8314
[5] Nebenführ B and Davidson L 2015 *Boundary-Layer Meteorology* 253–276 ISSN 0006-8314
[6] Shaw R H 1992 *Boundary Layer Meteorology* 47–64
[7] Da Costa J C, Castro F A and Santos C S 2017 *Energy Procedia* **136** 501–506 ISSN 18766102
[8] Brown K W and Covey W 1966 *Agricultural Meteorology* **3** 73–96
[9] Arnqvist J, Segalini A, Dellwik E and Bergström H 2015 *Boundary-Layer Meteorology* **156** 53–71 ISSN 1573-1472
[10] Öhlund O and Larsson C 2015 *Applied Acoustics* **89** 34 – 41 ISSN 0003-682X
[11] Boy M, Sogachev A, Lauros J, Zhou L, Guenther A and Smolander S 2011 *Atmospheric Chemistry and Physics* **11** 43–51
[12] Boudreault L É, Bechmann A, Tarvainen L, Klemedtsson L, Shendryk I and Dellwik E 2015 *Agricultural and Forest Meteorology* **201** 86–97 ISSN 01681923
[13] Olsen B 2018 *Mesoscale to microscale coupling for determining site conditions in complex terrain* Ph.D. thesis Denmark
[14] Lalic B and Mihailovic D T 2004 *Journal of Applied Meteorology* **43** 641–645
[15] Schröter J S, Moene A F and Holtslag A A M 2013 *Quarterly Journal of the Royal Meteorological Society* **139** 1694–1711 ISSN 00359009
[16] C K J and J F J 1994 *Atmospheric Boundary Layer Flows - Their Structure and Measurement* (Oxford University Press)
[17] Yi C, Monson R K, Zhai Z, Anderson D E, Lamb B, Allwine G, Turnipseed A A and Burns S P 2005 *Journal of Geophysical Research: Atmospheres* **110**
[18] Sogachev A, Menzhulin G V, Heimann M and Lloyd J 2002 *Tellus B: Chemical and Physical Meteorology* **54** 784–819
[19] Sogachev A, Dellwik E and Boegh E 2013 Evapotranspiration and heat fluxes over a small forest - a study using modelling and measurements *Climate and Land Surface Changes in Hydrology. Proceedings of H01, IAHS-IAPSO-IASPEI Assembly* (IAHS Press) pp 272–277 ISBN 978-1-907161-37-7
[20] Wilson K B, Baldocchi D D, Aubinet M, Berbigier P, Bernhofer C, Dolman H, Falge E, Field C, Goldstein A, Granier A, Grelle A, Halldor T, Hollinger D, Katul G, Law B E, Lindroth A, Meyers T, Moncrieff J, Monson R, Oechel W, Tenhunen J, Valentini R, Verma S, Vesala T and Wofsy S 2002 *Water Resources Research* **38** 30–1–30–11